Journal of
Fluid Mechanics and Mechanical Design

e-ISSN: 2582-9165
Volume-5, Issue-2 (May-August, 2023)

www.matjournals.com

Low Reynolds-Number Dependence on Aerodynamic Properties of a High-Performance Airfoil

Simaran Kumari*
Assistant Professor, Department of Mechanical Engineering, Meerut Institute of Technology, Meerut, Uttar Pradesh, India

*Corresponding Author: simaranshree@gmail.com

Received Date: August 29, 2023 *Published Date: September 08, 2023*

ABSTRACT

The High-performance, low-Reynolds-number airfoils with a high lift-to-drag ratio include the SD7003 and Ishii models. Despite extensive research on aerodynamic features at specific Reynolds numbers, research on how aerodynamic qualities are changed by Reynolds numbers that emerge for common low-Reynolds-number airfoils is limited. This study investigates the relationship between these two airfoils' aerodynamic efficiency and Reynolds number. The findings show that, in comparison to the SD7003 airfoil, the Ishii airfoil is especially less sensitive on the lift curve's Reynolds number. The lift slope seldom changes even when the Reynolds number changes, despite the fact that there is a little variation over the maximum lift coefficient for high angles of attack. When developing wind turbines or small aeroplanes, there has been a rise in interest in the previous NACA four-digit series. The NACA 0018 profile is one of the airfoils that are widely employed for this purpose. However, almost no additional experimental studies of this profile have been conducted since 1933, a period of more than 70 years, to examine its performance for a range of turbulence parameters and under the Low and medium Reynolds values regime. In this paper, the lift and drag coefficients of the NACA 0018 airfoil are studied in relation to the Reynolds number and the intensity of the turbulence.

Keywords- Aerodynamics, Ishii airfoil, Low-reynolds-number, Reynolds number dependence, Separation bubble

INTRODUCTION

Aerodynamically, chorded low Reynolds number airfoils Reynolds numbers operate effectively. Less than 105 are crucial (Re) [1]. The so-called "Mars aeroplane" has been the subject of extensive research and discussion in Japan. Low Reynolds number aircraft now have a new use that enables airborne research on Mars [2-5]. A Japanese research team completed a high-altitude flying demonstration test with the first fixed-wing Mars aircraft prototype in 2016 [6].

On the wing surface, separation bubbles form and burst in this region with low Reynolds number [1]. Physical processes of this nature result in non-linear lift curves and have an impact on what effect performance in terms of aerodynamics is the Reynolds number [6-8]. Reynolds number, angle of attack, and airfoil design all play major roles in it. As a result, physical aerodynamics is used in the high-performance wing design of low-Reynolds number aircrafts [9-10]. A lot of research has been done on the behaviour of separation bubbles on example symmetric airfoils like the flat plate and NACA0012. Other useful asymmetric airfoils are the Ishii airfoil and the Selig-Donovan (SD) 7003 airfoil. The aerodynamic properties are described because of their great performance at low Reynolds numbers. These two airfoils are considered airfoils with great performance because they have high lift-to-drag (L/D) ratios at low Reynolds numbers, below Re = 70,000. when the impact of the low Reynolds number becomes more apparent. Due to its high L/D at 20,000 Reynolds number cruising, the Ishii airfoil is specifically considered to be a potential contender for the Japanese Mars airplane's main-wing airfoil. Aono et al used large-eddy simulations to investigate the aerodynamic properties of these two airfoils at Re = 23,000. The airfoil on the upper surface, according to the findings, shape predominates both the

development of laminar separation bubbles and the change from laminar [2]. Although the flow-fields around the airfoils and aerodynamic qualities at various Although Reynolds numbers have been studied, it is still unclear how they affect aerodynamic qualities. Recognizing the impact of Reynolds number variations on aerodynamic performance, notably lift characteristics, is important because low-Reynolds number aircrafts, like Mars aeroplanes, may fly at a variety of heights and speeds. The impact of this study examines how Ishii and SD7003 airfoils' lift and drag properties are affected by Reynolds number. Along the anticipated path of the Japanese Mars plane, a transitive condition is one with a Reynolds number less than 23,000. Thus, from 23,000 to 60,000, the Reynolds number was modified. Additionally, the smoke-wire approach was used at Re = 23,000 to visualize the flow-field surrounding the airfoils.

EXPERIMENTAL SETUP AND CONDITIONS

Test model

Fig 1 displays the geometry of the SD7003 and Ishii airfoils, while Table 1 lists their characteristics. Although there are little modifications in the region of the maximum thickness, SD7003 has a somewhat bigger thickness than Ishii [4, 5]. Additionally, there isn't although the upper surface's geometry varies widely, the shape of the lower surface differs, particularly between x/c = 0.4 and 0.6, where the Ishii airfoil's under camber is strong and causes its camber to be greater than that of SD7003. The tiny leading edge radius of both airfoils is in line with the Schmitz-proposed high-performance low-Reynolds number airfoil's shape characteristics.

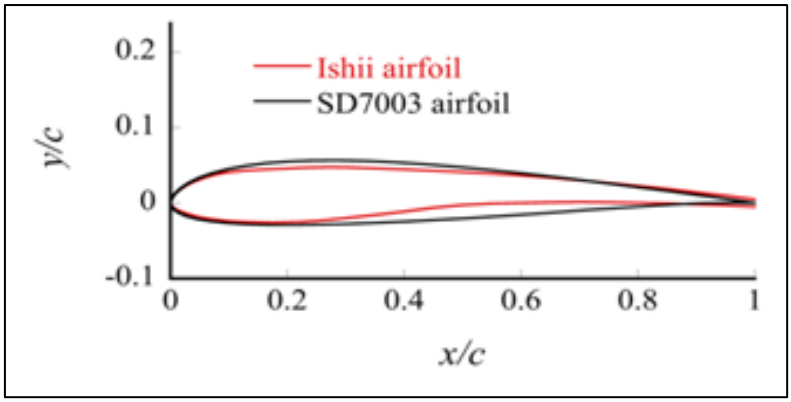

Figure 1: *Airfoil shape (Red line: Ishii airfoil, Black line: SD7003 airfoil).*

Table 1: *Geometric features of airfoils.*

	Maximum Thickness (%)	Location (x/c) of Maximum Thickness	Maximum Camber (%)
Ishii airfoil	7.1	0.25	2.3
SD7003 airfoil	8.5	0.24	1.5

Stereolithography polymers with high transmission are used to create both test models. The test models' chord and span lengths are respectively 80 mm and 180 mm.

Measurement of Aerodynamic Forces and Visualisation of Flow

At Kyushu University, we performed a number of tests utilising a Low-speed open-circuit wind tunnel. To reduce turbulence, Upstream of the contraction portion, four screens and a honeycomb were put in place. When moving at 5.0 m/s, the test section centre experienced turbulence with an intensity of roughly 0.3%. The entire experimental setup is shown in Fig. 2. The test portion had an acrylic sidewall covering on either side, and its rectangular cross-section was 180 mm by 360 mm. To measure the aerodynamic forces, the

parallel-to-the-ground test model was attached to a three-part technique for measuring micro-force balance (NISSHOELECTRIC-WORKS LMC-3501-5N). The balance system's for each coupled load, lift and drag forces were each 5 N, and the momentum was 0.5 Nm. The lift and drag forces were previously measured, thus the accuracy of the aerodynamic force measurement is assessed to be 0.2%. Less than 0.5% of the span length must separate the sidewall from the model tip and gaps between 0.1 and 1.4 mm are frequently acceptable and have no impact on the measurements of aerodynamic force, according to Burns et al. The gap was reduced to 0.5mm as a result of these observations. The identical test-model setup was used. It was used to make aerodynamic force measurements. Two 0.1-mm diameter nichrome wires were placed horizontally at the test portion and were covered in liquid paraffin. Smoke was produced by heating the wires using a voltage slider (S-130-10, Yamaha Electrics). The light source was a 2W green laser (SDL-532-2000T, Scitec Instruments Ltd.). After that, a high-speed video camera (Miro C110, Phantom) was used to capture the smoke line.

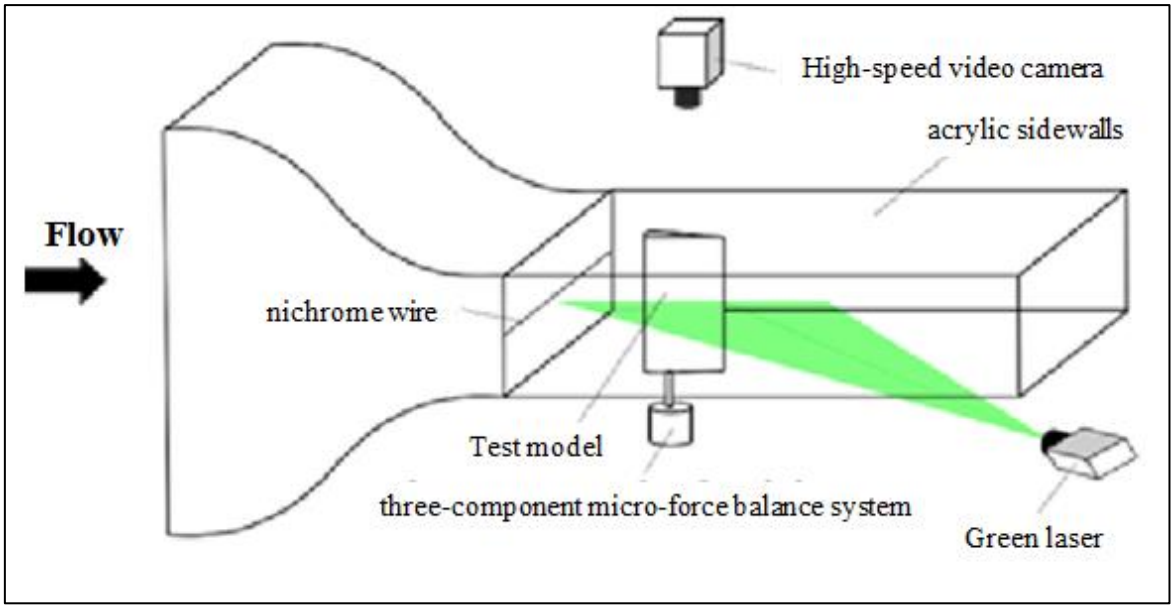

Figure 2: *Experimental setup.*

Experimental Conditions

The Reynolds number range based on chords of 23,000 to 60,000 was used to assess aerodynamic force. In 1° increments, attack angle (a) was increased from 10 to 15 degrees. For flow visualisation, on the top and bottom surfaces, only positive angles of attack at Re = 23,000 were employed. The fast-moving video camera has a frame rate of 400 frames per second and a shutter speed of 2,400 seconds. As a result, the camera's image resolution was 1280 by 1024 pixels.

RESULTS AND DISCUSSION

Aerodynamic Characteristics and Flow Field at Re =23,000

Fig. 3 contrasts the SD7003's lift, drag, and lift-to-drag ratios (L/D). From a = 2° to 4°, there is scarcely any difference in the lift curves. Fig. 3 compares the lift, drag, and lift- at Re = 23,000, the L/D of the SD7003 and Ishii airfoils. There is hardly any from a = 2° to 4° difference in the lift curves. However, it is evident that lift properties differ at both low and high attack angles. The SD7003 has a Maximum lift coefficient (CL max) of 0.75, compared to a CL max of 0.90 for the Ishii airfoil [6, 7]. Ishii airfoils have lower drag coefficients at positive angles of attack than at negative angles of attack. The SD7003 airfoil performs brilliantly. These results suggest that at positive angles of attack, the L/D of the Ishii airfoil is significantly larger than that of SD7003, and its maximum L/D (L/Dmax) is around 1.4 times that of SD7003. Our results are reasonable when compared to the Aono et al. It follows that the Ishii airfoil's lift and drag characteristics at Re = 23,000 are superior to those of SD 7003.

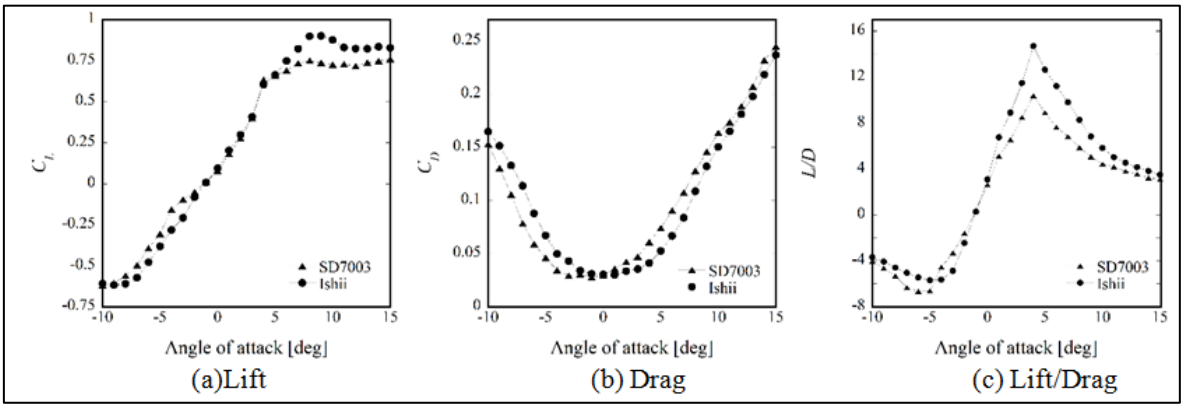

Figure 3: *Comparison of aerodynamic performance at Re =23,000.*

The visualisation @ Re = 23,000, results for the SD7003 and Ishii airfoils are shown in Fig. 4 and 5 respectively. According to the visualisation results Fig. 6 plots the upper surface's detachment and reattachment sites. The trailing edge separation occurs in the SD7003 airfoil's flow-fields shown in Fig. 4 at low angles. As the angle of attack increases, the point of separation advances upstream. At an angle of 3°, the separated shear layer begins to roll up and form a span-wise vortex along the trailing edge, corresponding to the separated shear layers laminar to turbulent transition. A separation bubble arises at a = 4° between the separation and reattachment sites as the divided shear layer rejoins the upper surface. As the angle of attack rises up to a = 8°, the separation bubble flows upstream [7-10]. We arrived to this conclusion that a leading edge separation exists. The flow adheres to the bottom surface at all attack angles. Fig. 5 and 6 demonstrate how the flow-field on the Ishii airfoil's upper surface is almost identical to that of SD7003 in Fig. 4. Despite the fact that the flow-fields are equivalent, the aerodynamic performance clearly differs, particularly at high angles of attack higher than 5°. This mismatch can be traced to the difference in pressure distribution on the bottom surface, which is caused by the lower surface's changing airfoil shape.

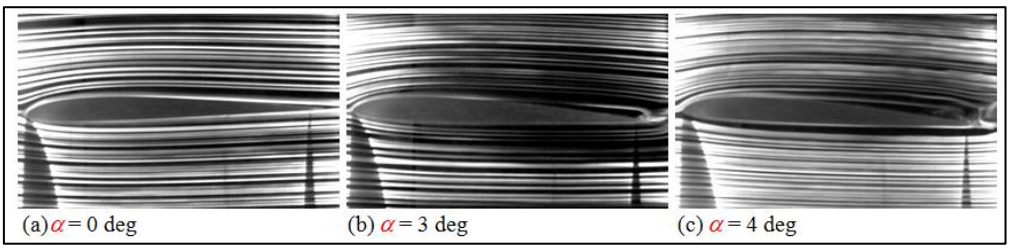

Figure 4: *Flow-field around SD7003 airfoil (Re = 23,000).*

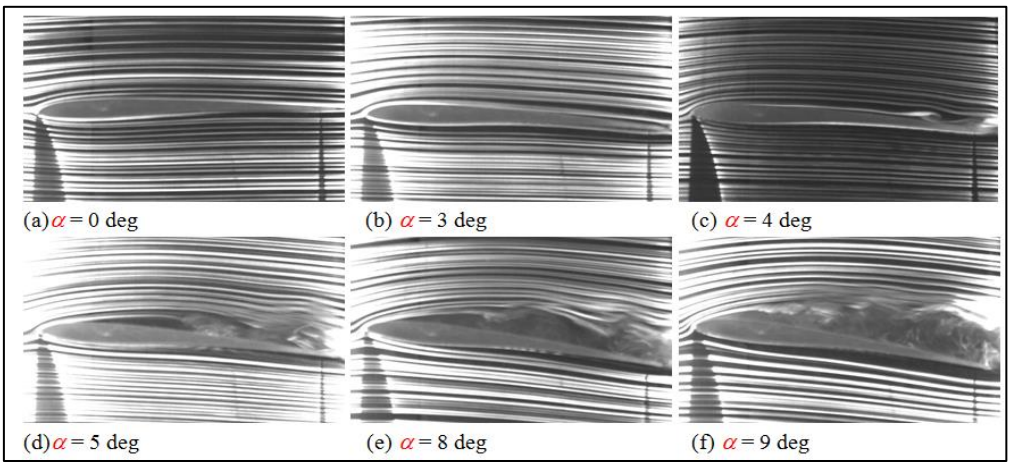

Figure 5: *Flow-field around Ishii airfoil (Re = 23,000).*

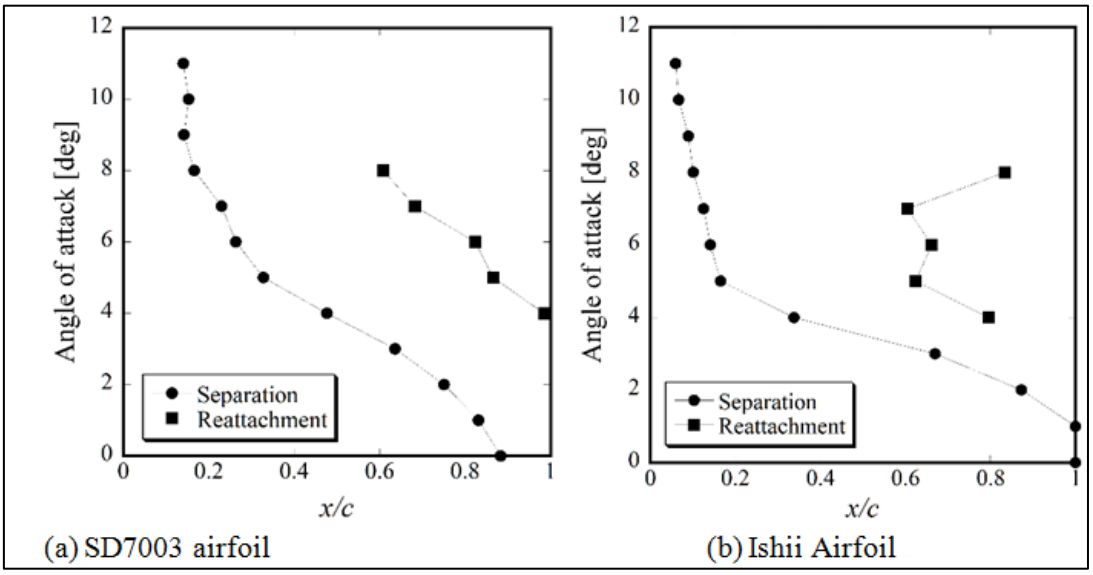

Figure 6: *Location of separation and reattachment points.*

CONCLUSION

This study looked at how the lift and drag characteristics of two high-performance low-Reynolds-number airfoils, Ishii and SD7003, are affected by Reynolds number. Aerodynamic experiments and flow visualizations were carried out when Reynolds numbers are low (Re = 23,000-60,000). Additionally, SD7003 outperforms SD7003 aerodynamically at all Reynolds numbers, and the Ishii airfoil has the lift curve and has a low reliance on Reynolds number. The visualisation findings for even after the separation bubble is formed upstream of the maximum thickness point, and the separation point remains stationary. To put it another way, the Ishii airfoil can fix close to the leading edge similarly to how a flat plate can fix close to a blunt leading edge. As a result, the Ishii airfoil is a high-performance, easy-to-control airfoil for Mars or other low-Reynolds-number aircraft in the Re = 23,000-60,000 region. All simulations performed for this investigation suggested a zero-lift coefficient at a zero angle of attack, regardless of the Reynolds number or degree of turbulence.

When there is a significant boundary layer laminar separation bubble, throughout the range of angles of attack before stall, two aerodynamic derivatives of the lift coefficient appear. The first section largely experiences a linear increase as the Reynolds number rises. In the second, the aerodynamic derivative zone, on the other hand, is essentially independent of the Reynolds number.

REFERENCES

1. J. C. Muti Lin and L L. Pauley (1996). Low-Reynolds-number separation on an airfoil, *AIAA Journal*, 34(8), Available at: https://arc.aiaa.org/doi/10.2514/3.13273.
2. G Bangga, A Dessoky, Z Wu, et al (2020). Accuracy and consistency of CFD and engineering models for simulating vertical axis wind turbine loads, *Energy*, 206, Available at: https://doi.org/10.1016/j.energy.2020.118087.
3. J M Ramírez and M Saravia (2021). Assessment of reynolds-averaged navier–stokes method for modeling the startup regime of a darrieus rotor, *Physics of Fluids*, 33, Available at: https://doi.org/10.1063/5.0045083.
4. E Branlard, I Brownstein, B Strom, et al (2022). A multipurpose lifting-line flow solver for arbitrary wind energy concepts, *Wind Energy Science*, 7, 455-467, Available at: https://wes.copernicus.org/articles/7/455/2022/.
5. J E Silva and L A M Danao (2021). Varying VAWT cluster configuration and the effect on individual rotor and overall cluster performance, *Energies*, 14(6), Available at: https://www.sciencegate.app/app/redirect#aHR0cHM6Ly9keC5kb2kub3JnLzEwLjMzOTAvZW4xNDA2MTU2Nw==.
6. K Rogowski, G Królak and G Bangga

(2021). Numerical study on the aerodynamic characteristics of the NACA 0018 airfoil at low reynolds number for darrieus wind turbines using the transition SST model, *Processes*, 9(3), Available at: https://doi.org/10.3390/pr9030477.

7. I Paraschivoiu (2002), Wind Turbine Design: With Emphasis on Darrieus Concept. *Presses inter Polytechnique*, Canada. ISBN: 2553009313, Available at: https://books.google.co.in/books/about/Wind_Turbine_Design.html?id=sefVtnVgso0C&redir_esc=y.
8. J Martinez, L Bernabini, O Probst and C Rodriguez (2005). An improved BEM model for the power curve prediction of stall-regulated wind turbines, *Wind Energy*, 8(4), 385-402, Available at: https://doi.org/10.1002/we.147.
9. M O. L. Hansen (2013), Aerodynamics of Wind Turbines. *Earthscan*, Oxfordshire, United Kingdom. ISBN: 1849770409, Available at: https://books.google.co.in/books/about/Aerodynamics_of_Wind_Turbines.html?id=GVD_HDPix6YC&redir_esc=y.
10. Z Zhang, S R K Nielsen, F Blaabjerg and D Zhou (2014). Dynamics and control of lateral tower vibrations in offshore wind turbines by means of active generator torque, *Energies*, 7(11), 7746-7772, Available at: https://doi.org/10.3390/en7117746.

CITE THIS ARTICLE

Simaran Kumari (2023). Low Reynolds-Number Dependence on Aerodynamic Properties of a High-Performance Airfoil, *Journal of Fluid Mechanics and Mechanical Design*, 5(2), 18-23.